Collective phase slips and phase synchronizations in coupled oscillator systems

Zhigang Zheng,[1,2] Bambi Hu,[2,3] and Gang Hu[1]
[1]*Department of Physics, Beijing Normal University, Beijing 100875, China*
[2]*Department of Physics and Center for Nonlinear Studies, Hong Kong Baptist University, Hong Kong, China*
[3]*Department of Physics, University of Houston, Houston, Texas 77204*
(Received 19 January 1999; revised manuscript received 26 January 2000)

Phase synchronization dynamics in coupled limit cycles with distributed natural frequencies are explored. A synchronization tree from free oscillations to local clustering and global phase locking is found. A desynchronization-induced transition to chaos is shown. Near the onset of various phase synchronization points, a simultaneous quantized stick-slip feature of the phases of oscillators is observed on the desynchronization side and heuristically interpreted in terms of a heteroclinic path instability.

PACS number(s): 05.45.Xt, 87.10.+e, 02.50.−r

I. INTRODUCTION

The dynamics of systems consisting of a large number of mutually interacting units is an intriguing problem in many fields, ranging from physics to chemistry, ecology, economics, and biology. A significant phenomenon among these behaviors is that a large population of interacting oscillators can spontaneously synchronize themselves to a common frequency, even if some quenched distribution of natural frequencies across the population exists [1,2]. This self-synchronization behavior can be found in laser arrays [3], Josephson-junction arrays [4], magnetic resonance processes (the coherent motion of magnetized domains in strongly coupled magnetic systems) [5], charged wave instabilities in plasma [6], and a large variety of chemical and biological systems [7–16]. A promising strategy in studying these systems is to adopt phase models [1,2]. A number of investigations have been made in the past few years on coupled limit cycle systems, where each system has periodic motion in the absence of coupling. Recently, the exploration has been extended to coupled chaotic systems. Under some circumstances one can define an appropriate phase of the individual chaotic oscillator [17], and the phase synchronization phenomenon has been found [18–20].

Although the mutual entrainment of coupled systems has been extensively explored, many intrinsic dynamical mechanisms are still unknown. For example, it is not clear how the various oscillators are led to complete synchronization via a sequence of transitions on increasing the coupling strength. It is important to elucidate this issue from a microscopic point of view. Recently, we studied this problem and found rich behaviors of synchronized bifurcations in coupled limit cycles [21]. In this paper we go further in exploring and understanding the essential features of the system. We consider the following set of N nonlinearly coupled phase oscillators with random natural frequencies ω_i taken from a normal Gaussian distribution $g(\omega)$ and with nearest coupling [1,2]:

$$\dot{\theta}_i = \omega_i + \frac{K}{3}[\sin(\theta_{i+1}-\theta_i)+\sin(\theta_{i-1}-\theta_i)]. \tag{1}$$

Here, $i=1,2,\ldots,N$, where K, θ_i, and $\dot{\theta}_i$ are the coupling strength, instantaneous phase, and velocity, respectively. $\theta_{i+N}(t)=\theta_i(t)$. Without losing generality we scale ω_i such that

$$\sum_{i=1}^{N} \omega_i = 0. \tag{2}$$

When one increases the coupling K, system (1) exhibits complicated synchronized dynamics due to the competition between the disorder originating from the quenched randomness of the natural frequencies of various oscillators and the order induced by the interaction among elements. For a given N and $\{\omega_i, i=1,2,\ldots,N\}$, there exists a critical coupling K_c when $K>K_c$ all oscillators can be phase locked to each other, one has $\{\dot{\theta}_i=0\}$ for $i=1,\ldots,N$, and each θ_i is locked to a fixed value. When the coupling strength K is lower than K_c, the oscillators cannot attain global phase locking, and then $\dot{\theta}_i(t)$ is nonzero and time dependent. It is found that if we define the average frequency of the ith oscillator as

$$\overline{\omega}_i = \lim_{T\to\infty} \frac{1}{T}\int_0^T \dot{\theta}_i(t)dt, \tag{3}$$

we may still observe a certain synchronization between different oscillators in the *time-averaged* sense, i.e., $\overline{\omega}_i = \overline{\omega}_j$ $(i\neq j)$ for the case $K<K_c$, when the strict phase locking $\dot{\theta}_i(t)=0$ is broken. In this regime, the system may exhibit complicated phase synchronization behaviors. It is an intriguing topic to investigate how these nonidentical limit cycles are led to complete synchronization on increasing the mutual coupling K from $K=0$.

The paper is arranged as follows. Section II is devoted to a general description of the synchronization process and the critical behavior near the onset of global phase locking. In Sec. III, we reveal a cascade of transitions for phase synchronization between oscillators or clusters of oscillators. The phase dynamics in the vicinities of these transitions are investigated. Bifurcation cascades from high-dimensional quasiperiodicity to chaos to low-dimensional quasiperiodicity and periodicity are explored in Sec. IV, where

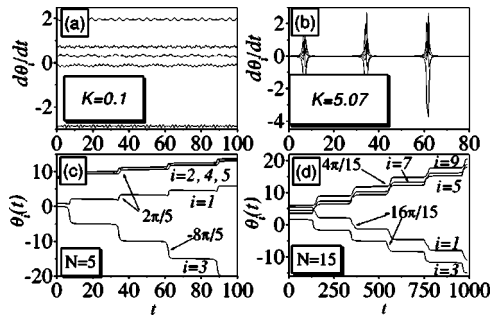

FIG. 1. (a),(b): The time evolutions of $\dot{\theta}_i(t)$ plotted for $N=5$ and two different coupling strengths $K=0.1$ and 5.07. Near the onset of the instability of the phase-locking state (b), simultaneous firings of all oscillators are clearly shown. (c),(d) The evolution of $\theta_i(t)$ plotted near the critical point $K=K_c$, where $K=5.07$, $N=5$ in (c) and $K=6.212$, $N=15$ in (d). Quantization of simultaneous phase slips for all oscillators is shown.

desynchronization-induced transitions to chaos are emphasized. We summarize our results in Sec. V.

II. SIMULTANEOUS PHASE SLIPS NEAR THE ONSET OF SYNCHRONIZATION

For N coupled oscillators, there exists a critical coupling strength K_c. If K is larger than K_c, all oscillators in the system are synchronized. It is interesting to study the dynamical behavior near the onset of global synchronization for K slightly smaller than K_c from a microscopic point of view.

It is natural to study the temporal behaviors of the rotating frequencies $\{\dot{\theta}_i(t)\}$ of the limit cycles. In Figs. 1(a) and 1(b), we present the evolutions of $\dot{\theta}_i(t)$ for $N=5$ and different coupling strengths. For $K=0$, $\dot{\theta}_i(t)$ must be equal to the constant natural frequency ω_i. For weak interactions among oscillators, $\dot{\theta}_i(t)$ varies in an oscillatory way around its natural frequency [Fig. 1(a)]. As K increases, the oscillation amplitude of $\dot{\theta}_i(t)$ becomes large, and at the same time the average frequencies $\overline{\omega_i}$ shift closer to each other from their individual natural frequencies ω_i. In Fig. 1(b), we plot the evolution of $\dot{\theta}_i(t)$ near the onset of synchronization, where we find simultaneous on-off oscillations, i.e., all oscillators stay in the phase-locking condition (off state) for a long time, and then simultaneous bursts (firings) of all oscillators (on state) break the locking state. After a short pulselike firing, all oscillators return simultaneously to the phase-locking state, and this process is repeated periodically. As K gets closer to K_c, the duration τ between two successive firings from the phase-locking state becomes longer, until at $K=K_c$, $\tau\to\infty$. In Figs. 1(c) and 1(d), the evolution of the phases of individual oscillators near the onset of global phase locking is plotted for $N=5$ and 15, and we find very characteristic quantized phase slips, i.e., the phase evolutions have a staircaselike shape. Oscillators stay at certain phase values for a long time and then simultaneously jump to new steps. The amplitudes of jumps for different elements may be different, e.g., in Fig. 1(c) for $N=5$, $\Delta\theta=2\pi/5$ for $i=1,2,4,5$ and $\Delta\theta=-8\pi/5$ for $i=3$, and in Fig. 1(d) for $N=15$, $\Delta\theta=4\pi/15$ for $i=5,7,9$ and $\Delta\theta=-16\pi/15$ for $i=1,3$. Moreover, a plot of duration τ against K_c-K shows a clear scaling relation

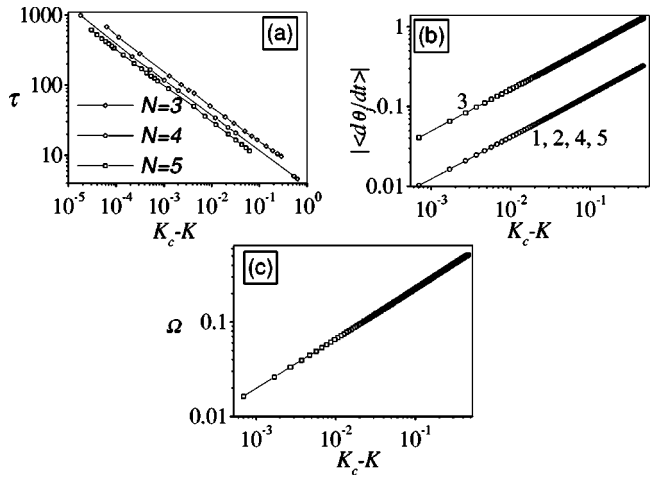

FIG. 2. (a) The log-log plot of the time τ between two phase slip firings and the coupling K_c-K for $N=3$, 4, and 5, and a scaling exponent of $-1/2$. (b) The absolute winding number for oscillators plotted against K_c-K for $N=5$; the absolute winding number of $i=3$ is four times larger than that of $i=1,2,4,5$ because of the relation Eq. (12). (c) The quantity Ω varying against K_c-K for $N=5$. For both (b) and (c), the scaling exponent is 1/2, indicating a typical saddle-node bifurcation from the phase-locking state.

$$\tau\propto(K_c-K)^{-1/2}, \tag{4}$$

as shown in Fig. 2(a) for $N=3$, 4, and 5.

These features (synchronized firings of motion and quantized slips of phase in each firing) can be understood by an intuitive interpretation. Suppose that various oscillators can be locked to a set of phases $\overline{\theta_i}(K)$ for $K>K_c$. Since the forces on the right-hand side of Eqs. (1) have 2π periodicity with respect to all the phase angles θ_i, $i=1,2,\ldots,N$, it is clear that all sets satisfying the relations

$$\begin{aligned}\Delta\overline{\theta}_{i+1}(K,\mathbf{m}) &= \overline{\theta}_{i+1}(K,\mathbf{m})-\overline{\theta}_i(K,\mathbf{m})\\ &= \overline{\theta}_{i+1}(K)-\overline{\theta}_i(K)+2\pi m_i\\ &= \Delta\overline{\theta}_i(K)+2\pi m_i\end{aligned} \tag{5}$$

must also be phase-locking solutions of Eq. (1). Where $\mathbf{m}=(m_1,\ldots,m_j,\ldots,m_N)$ and m_i is any integer. The phase-locking solutions may lose their stability via a saddle-node bifurcation when K is decreased to less than K_c. At the critical point $K=K_c$, there exists a heteroclinic path linking some of these phase-locking solutions, which has the lowest potential, and is attractive. For the particular case $N=2$, the existence of such a heteroclinic path can be rigorously proved [22]. Near the onset of desynchronization, i.e., $K<K_c$, and $|K-K_c|\ll 1$, the saddle-node instability leads to motion along this heteroclinic path. That is, the system takes such a periodic path, which stays in the vicinity of one of the above stationary solutions for a long time (''off'' state), escapes from this solution, and then quickly approaches the vicinity of the next stationary solution along the heteroclinic path $K=K_c$ (''on'' state, firing). Due to the interaction of units, all oscillators experience simultaneous phase slips, or,

say, synchronized firings. This mechanism leads to the simultaneous periodic pulses of Fig. 1(b). For the saddle-node bifurcation, we have a universal form [23]:

$$\dot{x}=(K_c-K)+x^2. \tag{6}$$

The time τ for x to move from $x=0$ to $x\to\infty$ reads

$$\tau\propto\int_0^\infty \frac{dx}{(K_c-K)+x^2}=\frac{\pi}{2\sqrt{K_c-K}}. \tag{7}$$

This explains the scaling relation (4). For this saddle-node bifurcation, we expect that $\overline{\omega_i}$ and $\Omega=\Sigma_{i=1}^{N}|\overline{\omega_i}|$ obey the typical scaling behavior: $|\overline{\omega_i}|\propto(K_c-K)^{1/2}$, $\Omega\propto(K_c-K)^{1/2}$. In Figs. 2(b) and 2(c), we give numerical results for the scaling in the critical regime for $N=5$, which are in good agreement with the above prediction.

Based on the above discussions, it is interesting to compute the phase slips of various oscillators during each phase slip pulse. Let $\Delta\theta_i$ denote the phase shift of θ_i during each firing. From Eqs. (2) and (3), we have

$$\sum_{i=1}^{N}\Delta\theta_i=0, \tag{8}$$

i.e., due to the absence of motion of the center of mass, the total shifts of various oscillators are zero. Thus, if there are limit cycles rotating in the clockwise direction, there must also exist elements rotating counterclockwise for balance. We further argue that any two adjacent fixed points along a heteroclinic path at $K=K_c$ take $m_i=0$ or ±1 in Eqs. (5), i.e.,

$$\Delta\theta_{i+1}-\Delta\theta_i=0 \quad \text{or} \quad \pm2\pi \tag{9}$$

for $i=1,2,\ldots,N-1$. Combining both the condition (8) and the hierarchy (9), one finds that $\Delta\theta_i$ takes only the following quantized values:

$$\Delta\theta_i=0,\pm\frac{2\pi}{N},\pm\frac{4\pi}{N},\ldots,\frac{2(N-1)\pi}{N},2\pi. \tag{10}$$

In realistic systems, the value for each $\Delta\theta_i$ depends on the choice of the distribution of $\{\omega_i\}$. Returning to Figs. 1(c) and 1(d), we find that the labeled phase shifts are completely consistent with Eq. (10). In fact, the shifts can be exactly worked out after we clarify the behavior of phase synchronization in the next section.

III. TRANSITION-TREE CASCADE OF PHASE SYNCHRONIZATIONS

From the microscopic point of view, it is significant to study how the competition between disorder and interactions leads to global entrainment of various oscillators. As we reduce K to values considerably smaller than K_c, no more phase locking exists, and no apparent synchronization can be observed directly for $\dot{\theta}_i(t)$. However, some other implicit synchronization—phase synchronization, which demands [24]

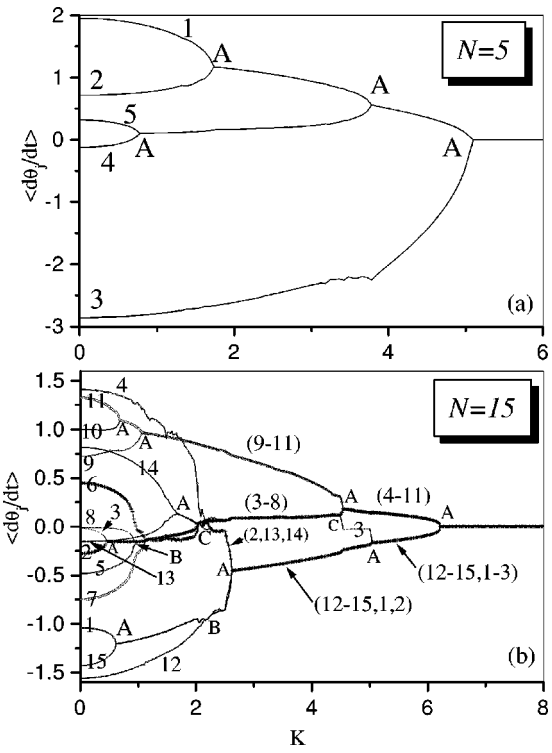

FIG. 3. Transition trees of synchronization for averaged winding numbers of various oscillators vs the coupling K. (a) $N=5$; (b) $N=15$. Different orders of clustering can be observed with the increase of K. Note the existence of three kinds of transitions labeled A, B, and C. The curves are based on numerical simulations for K step $\Delta K=0.01$. This is the same for Figs. 6 and 7.

$$|m\theta_i(t)-n\theta_j(t)|<\text{const} \tag{11}$$

—can still be observed, where m,n are two integers representing the $m:n$ phase locking. Obviously this phase locking is valid in an average sense. A typical case is 1:1 phase locking, which is equivalent to the condition $\overline{\omega_i}=\overline{\omega_j}$. In order to clearly show the hierarchy of phase locking among oscillators and the competition between the natural frequency distribution and the coupling intensity, we plot the $\overline{\omega_i}$-K curves to show the characteristics of various synchronizations. In Figs. 3(a) and 3(b), we plot $\overline{\omega_i}$ defined in Eq. (3) against K for $N=5$ and 15, respectively, by varying K from $K=0$ to $K>K_c$. In both figures, we find transition trees of phase synchronizations.

A systematic investigation of Figs. 3 shows that three kinds of transitions can be observed in the trees. First, if two lattice-adjacent oscillators (e.g., 1 and 2 are lattice adjacent, while 1 and 3 are not if $N\geqslant4$) or adjacent clusters of oscillators (here a *cluster* is defined as a group of oscillators with an identical average frequency) have close frequencies, they can easily be synchronized by increasing the coupling K. In this case, one always finds two branches merging to a single one (indicated by A). This kind of transition can be observed frequently along the bifurcation tree. Second, if two nonadjacent oscillators have close frequencies while the oscillators between them have considerably different frequencies, the nonadjacent oscillators can also become phase synchronized to each other, i.e., nonlocal clusters can be formed, and these nonlocal clusters can quickly bring the oscillators between

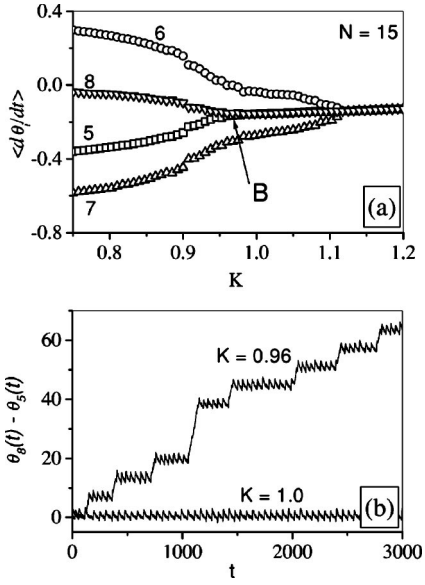

FIG. 4. (a) An enlarged plot of the nonlocal phase synchronization for $N=15$. (b) The time evolution of the phase difference $\theta_8(t)-\theta_5(t)$ before and after nonlocal phase synchronization.

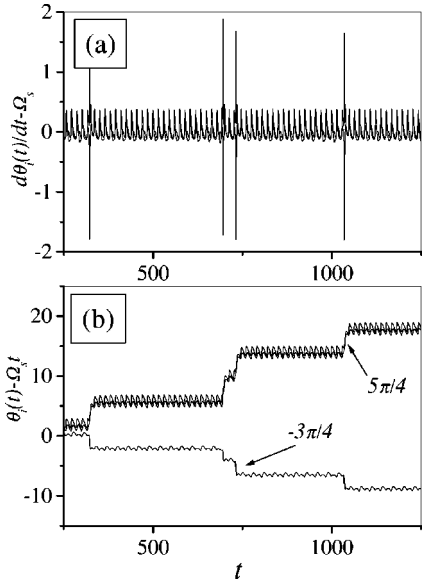

FIG. 5. (a): Synchronized firing of $\dot{\theta}_i(t)-\Omega_s$ at $K=4.534$ for $N=15$, where a cluster (4–11) desynchronizes to (4–8) and (9–11). Here $\Omega_s=0.182$ is the winding number at the transition point. (b) The evolution of the corresponding phase shift of $\theta_i(t)-\Omega_s t$.

them to the synchronized state and form a larger synchronized cluster. This kind of transition occurs frequently for systems with a large number of nonidentical elements, which are labeled B in Fig. 3(b). In Fig. 4(a), we give an enlarged plot of an example of type B bifurcation for the case $N=15$. Although oscillators 5 and 8 are nonadjacent, they become phase synchronized at about $K=0.99$. This nonlocal synchronization quickly brings the adjacent oscillator to a synchronized state, e.g., at $K=1.11$, this nonlocal cluster synchronizes with the sixth and seventh oscillators. In Fig. 4(b), we show the time evolution of the phase difference $\theta_8(t)-\theta_5(t)$ slightly before and after phase synchronization. Before the nonlocal locking occurs, one observes irregular phase slips of the phase difference. When phase synchronization takes place, the phase difference becomes localized, i.e., it oscillates around some value, and no phase slips between these two oscillators are found. This proves the existence of nonlocal phase synchronization. An oscillator that is synchronized to a cluster for a certain K may become desynchronized from the original cluster on increasing K. It is clear that this kind of transition is an inverse process of synchronization. This desynchronization always happens at the edge oscillator of a cluster, due to the competition between two neighboring clusters [labeled C, e.g., see the second and third oscillators of Fig. 3(b)]. Transitions of type A are normal, but B and C are different types of transitions.

Based on the bifurcation tree presented in Fig. 3, we are able to exactly explain the phase shifts in Figs. 1(c) and 1(d). For the case of $N=5$, when $K<K_c$ and $|K-K_c|\ll 1$, one has two clusters 3 and 1, 2, 4, 5. Thus, from the relation (9), we have

$$\sum_{1,2,4,5}\Delta\theta_i=-\Delta\theta_3=4\Delta\theta_i, \tag{12}$$

where $i=1,2,4,5$. Because oscillators 2 and 3 belong to different clusters, and $\bar{\omega}_2>0$, $\bar{\omega}_3<0$, one has from the condition (9)

$$\Delta\theta_2-\Delta\theta_3=2\pi.$$

By solving the above equations, it is easy to obtain $\Delta\theta_3=-8\pi/5$ and $\Delta\theta_i=2\pi/5$, $i=1$, 2, 4, and 5. For $N=15$, we have two clusters near K_c, i.e., the clockwise cluster (4–11) and the anticlockwise cluster (1–3,12–15). Thus from Eq. (8) we get

$$\sum_{4-11}\Delta\theta_i=8\Delta\theta_i=-\sum_{1-3,12-15}\Delta\theta_j=-7\Delta\theta_j, \tag{13}$$

where $i=4$–11 and $j=1$–3,12–15. Similarly $\Delta\theta_3-\Delta\theta_4=-2\pi$. These equations thus lead to $\Delta\theta_i=14\pi/15$ for $i=4$–11 and $\Delta\theta_j=-16\pi/15$ for $j=1$–3 and 12–15. This analysis indicates that the phase shifts of oscillators relate closely to the final clusters. For a general case, assuming that there are N_1 $(N-N_1)$ clockwise (anticlockwise) oscillators, a similar treatment to the above argument leads to

$$\Delta\theta_i=\frac{2\pi(N-N_1)}{N} \tag{14}$$

for the clockwise cluster and

$$\Delta\theta_j=-\frac{2\pi N_1}{N} \tag{15}$$

for the anticlockwise cluster.

An interesting fact is that the stick-slip feature and the related quantized phase shifts in firing pulses can be observed at other high-order transitions in the cascade tree of Fig. 3. For instance, in Fig. 5(a), we plot the phase dynamics for $K=4.534$ and $N=15$, where one large synchronized cluster (4–11) desynchronizes to two clusters (4–8) and (9–11). A stick-slip feature with simultaneous firing is found, and the phase shifts during each firing are shown in Fig. 4(b), which can be analytically computed by using the technique of Eqs.

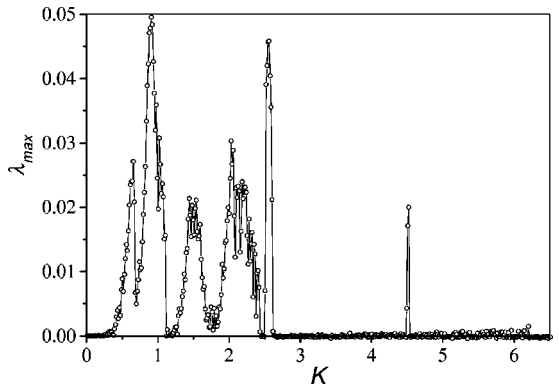

FIG. 6. The maximum Lyapunov exponent $\lambda_{\max}$ plotted against the coupling K for $N=15$. In a large regime, $\lambda_{\max}>0$, indicating chaos.

(12)–(15). Similar behavior is confirmed at other transitions, like $K=5.02$, 2.6, 1.06, and 0.66 in Fig. 3(b).

IV. BIFURCATION FROM QUASIPERIODICITY TO CHAOS AND PERIODICITY

In previous sections, we concentrated on the average behavior of the coupled oscillators. From an average point of view, the route from desynchronization to global phase locking is a transition tree of different orders of synchronizations, as shown in Figs. 3. As some average winding numbers become locked, i.e., $\overline{\omega_i}=\overline{\omega_j}$, the dimensionality of the coupled system decreases. However, due to the couplings among oscillators, the actual dynamics without averaging can be very complicated, i.e., the motion in the synchronization trees of Fig. 3 may be very different. It can be periodic, quasiperiodic and even chaotic. the dynamic features along these synchronization trees. In Fig. 6, we consider the case of $N=15$ and plot the largest Lyapunov exponent $\lambda_{\max}$ of the system against the coupling strength K. We find that, in a large interval of K, the maximum Lyapunov exponent is positive, indicating chaos. Therefore, in this region phase synchronizations of chaotic oscillators are identified. Recently, the phase synchronization of coupled chaotic systems has attracted great attention, and clustering, synchronization, and other collective behaviors have been explored. An essential difference between the previous chaos synchronization and ours is that in the latter case individual oscillators are periodic in the absence of coupling, and chaos is induced by nonlinear interactions of periodic oscillators, while in the former case the individual units are intrinsically chaotic without coupling.

It is interesting to see how chaos is generated in these systems. In Figs. 7, we give the correspondence between the bifurcation tree of phase synchronizations and the maximum Lyapunov exponent at some characteristic intervals. It is clearly shown that chaos occurs before a new phase synchronization is attained or a desynchronization happens. For example, for $K=2.415$–2.4, a large cluster desynchronizes to smaller ones, the motion of the system becomes irregular, and one then observes a positive Lyapunov exponent. For $K=2.5$–2.61, the cluster of sites (1,2,12–15), of which the motion is quasiperiodic with the largest Lyapunov exponent being zero, bifurcates to two clusters (2,13,14) and (1,12,15),

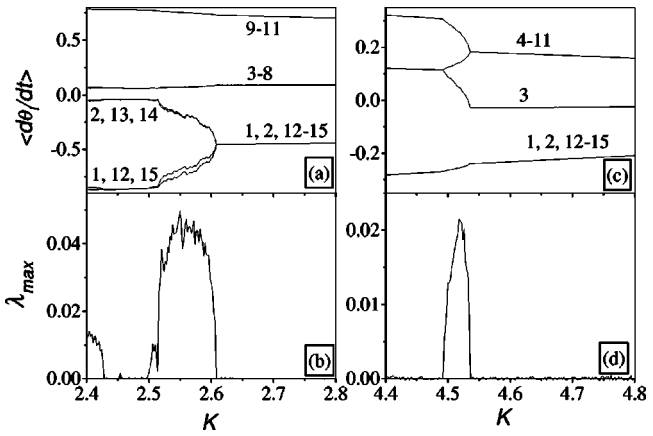

FIG. 7. Enlarged plot of the transition tree of average frequencies and the corresponding behavior of $\lambda_{\max}$ for $N=15$. Positive $\lambda_{\max}$ are observed when clustering or declustering occurs.

and we then find positive $\lambda_{\max}$ after desynchronization. A similar phenomenon can be observed for $K=4.49$–4.54, when the edge oscillator 3 desynchronizes from the (3–8) cluster. Therefore, we call this transition desynchronization-induced chaos. This transition is reasonable because in both Figs. 7(a) and 7(c) the third irreducible frequency appears from the two-frequency quasiperiodicity due to the desynchronization effect, which induces the transition from quasiperiodicity to chaos (zero Lyapunov exponents to positive ones) in Figs. 7(b) and 7(d), respectively.

In Figs. 8(a) to 8(e), we plot the maps of $\dot{\theta}_1(n)$ to $\dot{\theta}_1(n$

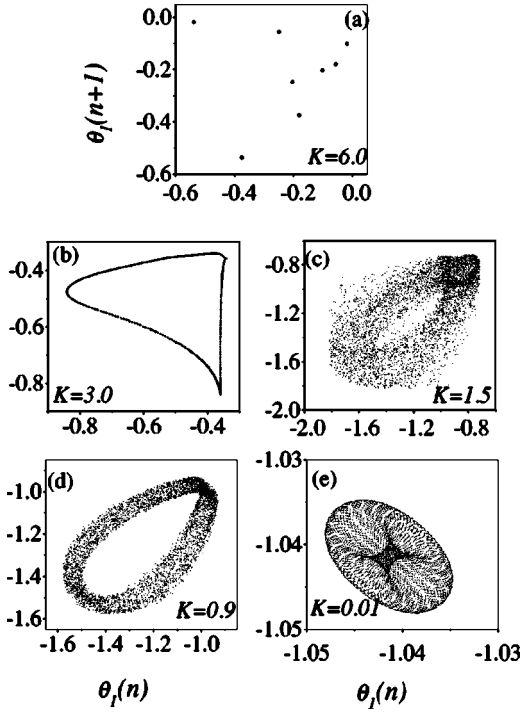

FIG. 8. Maps of $\dot{\theta}_1(n)$ to $\dot{\theta}_1(n+1)$ for $K=6.0$, 3.0, 1.5, 0.9, and 0.01 from (a) to (e), respectively. For $K=6.0<K_c=6.22$, period-8 motion is identified in (a). In (b) and (d), chaotic motions take place. (c) and (e) correspond to quasiperiodic tori, the dimension in (e) being much higher than in (c) [in (c), the torus is two dimensional].

$+1)$, where $\dot{\theta}_1(n)$ is the value of $\dot{\theta}_1(t)$ at the time t when $\theta_1(t)$ crosses the angle $2n\pi$ with n being an integer. When $K>K_c$, we obviously have a fixed point solution, and the map is fixed at $\dot{\theta}_1(n)=\dot{\theta}_1(n+1)=0$. For K slightly smaller than K_c, we have a periodic solution represented by a finite number of dots in Fig. 8(a). In 8(a), there are a total of eight dots, indicating a period-8 motion. From Fig. 3(b), we identify this as a two-cluster state, where the clusters are (4–11) and (1–3,12–15). From Fig. 1(d), this period-8 behavior can easily be understood. The period of the total system is 15τ, where τ is the time between two adjacent firings. The change of θ_1 in 15τ is 16π, because in each τ the slip amplitude of θ_1 is $-16\pi/15$, as seen from Fig. 1(d). Therefore one gets period-8 motion in Fig. 8(a). If one chooses the Poincaré map for the other cluster (4–11), it can easily be proved that the motion should be of period-7. Moreover, the periodicity of the motion of an oscillator depends on the cluster it belongs to. Generally, if there are N_1 oscillators in one cluster (denoted by $C1$) and $N-N_1$ in another ($C2$), the motion of the oscillator in $C1$ is period $(N-N_1)$, and the motion of oscillators in $C2$ is period N_1. A two-frequency torus can be identified in the three-cluster regime [see Fig. 7(b)]. This can be understood from Fig. 3(b); we have $6\overline{\omega}_1+6\overline{\omega}_3+3\overline{\omega}_9=\Sigma_{i=1}^{N}\omega_i=0$, indicating that only two average frequencies are linearly independent. For very small K, we can find high-dimensional quasiperiodicity [see, for example, Fig. 8(e)]. Between these two quasiperiodic regimes, chaos prevails [see Figs. 8(c) and 8(d), and the positive Lyapunov exponent regime in Fig. 6], and in this regime phase synchronization of chaotic oscillators and clusters takes place.

The entire variation from high-dimensional quasiperiodicity (for very weak coupling K) to periodic motion ($K<K_c$, $|K-K_c|\ll 1$) through various orders of chaos synchronization can be vividly seen in Figs. 3, 6, and 8. Starting from the high-dimensional quasiperiodicity for $K\ll 1$, on increasing K various neighboring oscillators with close frequencies start to form clusters via phase synchronization, and chaos is induced near the first synchronization. Then in each cluster different oscillators perform different chaotic motions, while possessing an identical winding number. The winding numbers for different clusters are different. On further increasing K, adjacent chaotic clusters can be synchronized to form larger clusters, until two large clusters are formed, when the motion becomes periodic. A cascade of transitions from high-dimensional to low-dimensional quasiperiodic tori is observed, which are regular quasiperiodic windows embedded in chaotic motion. This relates to the process of phase synchronization among various oscillators and clustering. This tree picture of transitions is expected to be common in general for a large number of coupled nonidentical oscillators, that are periodic in the uncoupled case.

V. CONCLUDING REMARKS

In this paper, we explored the phase synchronization dynamics in locally coupled limit cycles with distributed natural frequencies. We found a synchronization tree from free oscillations to local clustering and to global phase locking, and a change from high-dimensional quasiperiodic tori for weak coupling strength to low-dimensional quasiperiodicity and periodic motions (near the onset of phase locking) through various orders of chaotic phase synchronization. Chaos and periodic windows occur during the transitions from high- to low-dimensional quasiperiodic tori. In a synchronized cluster, the motions of oscillators are different, but they have an identical winding number. Chaos occurs frequently near the onset of phase synchronization. We also found several different types of phase synchronizations. The complicated bifurcation tree is the consequence of competition between the quenched disorder of natural frequencies and the collective tendency induced by the coupling, and the competition between the interaction distance and the natural frequency differences. Near the onset of various phase synchronization transitions and of global phase locking, we find a simultaneous stick-slip behavior of the phases of all oscillators. The instantaneous phase velocities of various oscillators exhibit a firinglike feature. In these regimes, the oscillators also exhibit collectively quantized phase slips. By using a heteroclinic orbit argument, we gave these critical behaviors intuitive interpretations, and the quantized phase slips are well predicted.

Although the discussion in this paper is based on the particular model of Eqs. (1), the rich synchronization behaviors found are expected to be observable in general coupled systems that have distributed frequencies and are periodic individually in the absence of coupling.

ACKNOWLEDGMENTS

This work is supported in part by the Research Grant Council (RGC) and a Hong Kong Baptist University Faculty Research Grant (FRG), and in part by the National Natural Science Foundation of China, the Special Funds for Major State Basic Research Projects, and the Foundation for Doctoral Training of the State Education Ministry of China.

[1] Y. Kuramoto, *Chemical Oscillations, Waves, and Turbulence* (Springer-Verlag, Berlin, 1984).
[2] A. T. Winfree, *Geometry of Biological Time* (Springer-Verlag, New York, 1990).
[3] H. Haken, *Advanced Synergetics* (Springer-Verlag, Berlin, 1983).
[4] T. D. Clark, Phys. Lett. **27A**, 585 (1968); R. Bonifacio *et al.*, *ibid.* **101A**, 427 (1984); D. R. Tilley, *ibid.* **33A**, 205 (1970); K. Wiesenfeld *et al.*, Phys. Rev. Lett. **76**, 404 (1996).
[5] F. Ritort, Phys. Rev. Lett. **80**, 6 (1998).
[6] S. Ichimaru, *Basic Principles of Plasma Physics: A Statistical Approach* (Addison-Wesley, Reading, MA, 1980).
[7] A. H. Cohen, P. J. Holmes, and R. H. Rand, J. Math. Biol. **13**, 345 (1982).
[8] N. Kopell and G. B. Ermentrout, Commun. Pure Appl. Math. **39**, 623 (1986).
[9] S. H. Strogatz and R. E. Mirollo, J. Phys. A **21**, L699 (1988); Physica D **31**, 143 (1988).
[10] L. Glass and M. C. Mackey, *From Clocks to Chaos, The Rhythm of Life* (Princeton Univ. Press, Princeton, NJ, 1988).
[11] C. Schafer *et al.*, Nature (London) **392**, 239 (1998).
[12] P. Tass *et al.*, Phys. Rev. Lett. **81**, 3291 (1998).

[13] J. Buck and E. Buck, Sci. Am. **234**, 74 (1976); J. Buck, Q. Rev. Biol. **63**, 265 (1988).
[14] T. J. Walker, Science **166**, 891 (1969).
[15] R. D. Traub, R. Miles, and R. K. S. Wong, Science **243**, 1319 (1989).
[16] M. K. McClintock, Nature (London) **229**, 244 (1971).
[17] T. Yalcmkaya and Y. C. Lai, Phys. Rev. Lett. **79**, 3885 (1997).
[18] M. Rosenblum, A. S. Pikovsky, and J. Kurths, Phys. Rev. Lett. **76**, 1804 (1996); G. V. Osipov, A. S. Pikovsky, M. G. Rosenblum, and J. Kurths, Phys. Rev. E **55**, 2353 (1997).
[19] M. G. Rosenblum, A. S. Pikovsky, and J. Kurths, Phys. Rev. Lett. **78**, 4193 (1997).
[20] E. Rosa, Jr., E. Ott, and M. H. Hess, Phys. Rev. Lett. **80**, 1642 (1998); K. J. Lee, Y. Kwak, and T. K. Lim, *ibid.* **81**, 321 (1998).
[21] Z. Zheng, G. Hu, and B. Hu, Phys. Rev. Lett. **81**, 5318 (1998).
[22] For $N=2$, Eqs. (1) can be reduced to $\Delta\dot{\theta}(t)=2\omega_1-\frac{4}{3}\sin[\Delta\theta(t)]$, $\Delta\theta(t)=\theta_1-\theta_2(t)$. Then the phase-locking condition is $K=3|\omega|/2$. When $K>3|\omega|/2$, there are two phase-locking solutions $\Delta\bar{\theta}_s(K)=\arcsin[3|\omega|/(2K)]$ and $\Delta\bar{\theta}_u(K)=\pi-\arcsin[3|\omega|/(2K)]$; the former is stable while the latter is unstable. Due to the periodicity of $\sin(\Delta\theta)$, the sets of $\Delta\bar{\theta}_{s,u}(K,m)=\Delta\bar{\theta}_{s,u}(K)+2\pi m$ with m being any integer are the phase-locking solutions of Eqs. (1). As K is reduced to $K=3|\omega|/2$, a saddle-node bifurcation occurs place at $\Delta\bar{\theta}_s=\Delta\bar{\theta}_u=\pi$, and heteroclinic orbits linking $\Delta\theta=(2m-1)\pi$ and $\Delta\theta=(2m+1)\pi$, $m=\ldots,-2,-1,0,1,2,\ldots$, appear at the bifurcation point $K=3|\omega|/2$. This picture can be extended to the case of Eq. (1), though the latter case is more complicated and it is impossible to compute the explicit form of the heteroclinic orbits.
[23] Y. Pomeau and P. Maneville, Commun. Math. Phys. **74**, 189 (1980).
[24] G. Hugenii, *Horoloquim Oscilatorium* (Parisüs, Paris, 1673).